united nations
educational, scientific
and cultural
organization

international atomic
energy agency

the
abdus salam
international centre for theoretical physics

ICTP 40th Anniversary

SMR/1567 - 2

WORKSHOP ON

QUANTUM SYSTEMS OUT OF EQUILIBRIUM

(14 – 25 June 2004)

" The role of dissipation in the reentrant behavior associated with the Berezinskii Kosterlitz Thouless transition of two-dimensional Josephson junction arrays "

presented by:

V. Tognetti

Università di Firenze
Italy

THE ROLE OF DISSIPATIONN IN THE REENTRANT BEHAVIOR ASSOCIATED WITH THE BEREZINSKII KOSTERLITZ THOULESS TRANSITION OF TWO-DIMENSIONAL JOSEPHSON JUNCTION ARRAYS.

Valerio Tognetti [2,3,4].

.....

In collaboration with:

Luca Capriotti, [1], Alessandro Cuccoli, [2,3], Andrea Fubini, [2,3], and Ruggero Vaia [5,3]

[1]*Kavli Institute for Theoretical Physics, University of California, Santa Barbara, CA 93106*

[2]*Dipartimento di Fisica dell'Universitą di Firenze, Via G. Sansone 1, I-50019 Sesto Fiorentino (FI), Italy*

[3]*Istituto Nazionale per la Fisica della Materia, UdR Firenze, Via G. Sansone 1, I-50019 Sesto Fiorentino (FI), Italy*

[4]*Istituto Nazionale di Fisica Nucleare, Sezione di Firenze, Via G. Sansone 1, I-50019 Sesto Fiorentino (FI), Italy*

[5]*Istituto di Fisica Applicata "N. Carrara" del CNR, Via Madonna del Piano, 1, I-50019 Sesto Fiorentino (FI), Italy*

1. Introduction

A variety of condensed-matter systems with an intermediate (*mesoscopic*) scale have been recently developed. The characteristic quantum effects involving a macroscopic number of particles cause peculiar properties of all such devices, which make them appealing for applications. However the sizeable dimension of the devices implies that the relevant dynamical variables have to be considered as coupled to a very large (infinite) number of degrees of freedom of the surrounding *environment* (or *dissipation bath*). In these open systems, interaction with the environment leads in general to dissipation and decoherence which strongly affect the behavior of the system. It is thus es-

sential to study both quantum and dissipative effects. Two-dimensional (2D) arrays of nanosized Josephson junctions, both unshunted [1] and shunted [2] can indeed be produced, giving the opportunity to experimentally test the effects of dissipation.

2. Path Integral Monte Carlo for dissipative systems

The quantum dissipation is usually addressed within the Caldeira-Leggett (CL) framework [3]. Dissipation is described in terms of a linear coupling of the system with a bath of harmonic oscillators [4–6]. The path integral expression of the partition function of a quantum dissipative system,

$$\mathcal{Z} = \oint \mathcal{D}[\boldsymbol{q}]\, e^{-S[\boldsymbol{q}]}\,, \tag{1}$$

is given by the Euclidean action

$$S[\boldsymbol{q}] = \int_0^{\beta\hbar} \frac{du}{\hbar} \left[\frac{1}{2}\, \dot{\boldsymbol{q}}(u)\, \boldsymbol{A}\, \dot{\boldsymbol{q}}(u) + V\big(\boldsymbol{q}(u)\big) \right] + S_{\rm d}[\boldsymbol{q}]\,. \tag{2}$$

The effects of dissipation are contained in the influence action,

$$S_{\rm d}[\boldsymbol{q}] = \frac{1}{2\hbar} \int_0^{\beta\hbar} du \int_0^{\beta\hbar} du'\, \boldsymbol{q}(u)\, \boldsymbol{K}(u-u')\, \boldsymbol{q}(u')\,. \tag{3}$$

Here, $\boldsymbol{q} \equiv \{q_i\}_{i=1,\ldots,M}$ denotes the vector whose components are the M coordinates of the investigated system and $\boldsymbol{A} \equiv \{A_{ij}\}$ is the mass matrix. The kernel $\boldsymbol{K}(u) \equiv \{K_{ij}(u)\}$ is an $M \times M$ matrix, which is in general non local both in space and imaginary time. It depends on the temperature $T = (k_{\rm B}\beta)^{-1}$, is a symmetric and periodic function of the imaginary time u, $\boldsymbol{K}(u) = \boldsymbol{K}(-u) = \boldsymbol{K}(\beta\hbar - u)$, with vanishing average over a period.

When Josephson junction arrays (JJA) are considered, the influence action (2) is a good description of dissipative effects due to currents flowing to the substrate or through shunt resistances [7]. For such systems, an alternative dissipative mechanism due to radiative effects of the electromagnetic field was also recently suggested [8, 9]. This leads to a so called *anomalous* (or p-coupling) dissipation [10] , where the influence action (2) is replaced with:

$$S_{\rm ad}[p(u)] \int_0^{\beta\hbar} \frac{du}{2\hbar} \int_0^{\beta\hbar} \frac{du'}{\beta\hbar}\, \boldsymbol{p}(u)\, \boldsymbol{K}(u-u')\, \boldsymbol{p}(u')\,, \tag{4}$$

where $\boldsymbol{p}$ is the M-component vector of the momenta canonically conjugated to the coordinates $\boldsymbol{q}$. The physical consequences of the two different types of dissipation were investigated and discussed in Refs. [6, 11] by the effective potential method [12]. The relevant difference is that standard dissipation

quenches the quantum fluctuations of the coordinates, driving their behaviour towards the classical one, while the anomalous dissipation has an opposite effect, enhancing the quantum fluctuations of $\boldsymbol{q}$.

The standard path-integral Monte Carlo (PIMC) method, for computing the integral in Eq. (1), divides the imaginary-time interval $[0, \beta\hbar]$ into P slices of width $\varepsilon = \beta\hbar/P$ where P is called *Trotter number*. The partition function $\mathcal{Z}$ is obtained as the $P \to \infty$ extrapolation of

$$\mathcal{Z}_P = C\beta^{-\frac{MP}{2}} \prod_{i=1}^{M} \int dq_{i0} \int \prod_{\ell=1}^{P-1} dq_{i\ell}\, e^{-S_P[\{\boldsymbol{q}_\ell\}]}\,, \tag{5}$$

where the path $\boldsymbol{q}(u)$ turns into the P discrete quantities $\boldsymbol{q}_\ell = \boldsymbol{q}(\ell\varepsilon)$, and $\dot{\boldsymbol{q}}(u) \to (P/\beta\hbar)(\boldsymbol{q}_\ell - \boldsymbol{q}_{\ell-1})$; $S_P[\{\boldsymbol{q}_\ell\}]$ represents the discretized form of the action (2) and C is a temperature-independent normalization.

The application of the standard PIMC approach to dissipative systems is made difficult by the fact that the kernel $\boldsymbol{K}(u-u')$ is a non local (and long ranged) function of the imaginary time, [5]. Fourier path-integral approaches [13], possibly supported by the partial-averaging scheme [14] can perform better: however, the evaluation of the integral over the continuous path they still involve is a serious shortcoming in the case of many-body systems.

Recently, we have proposed [15] to start from the finite-P expression (5) of the standard PIMC for the partition function and make there a lattice (discrete) Fourier transform, changing the integration variables from $q_{i\ell}$ to q_{ik} by setting:

$$\boldsymbol{q}_\ell = \bar{\boldsymbol{q}} + \sum_{k=1}^{P-1} \boldsymbol{q}_k\, e^{i\,2\pi\ell k/P}\,, \tag{6}$$

so that the discretized partition function reads:

$$\mathcal{Z}_P = C\beta^{-\frac{PM}{2}} \prod_{i=1}^{M} \int d\bar{q}_i \int \prod_{\ell=1}^{P-1} dq_{ik} \tag{7}$$

$$\times \exp\left\{ - \sum_{k=1}^{P-1} \boldsymbol{q}_k \left[\frac{2P^2}{\beta\hbar^2} \sin^2 \frac{\pi k}{P} \boldsymbol{A} + \frac{\beta}{2} \boldsymbol{K}_k \right] \boldsymbol{q}_k^* - \frac{\beta}{P} \sum_\ell V(\boldsymbol{q}_\ell) \right\},$$

where $\boldsymbol{K}_k \equiv \{K_{ij,k}\}$ is the Matsubara transform of the dissipation kernel matrix at the Matsubara frequency $\nu_k = 2\pi k/\beta\hbar$.

In order to get a reliable estimate of statistical averages in the thermodynamic limit ($M \to \infty$), finite-size effects have to be negligible; as a consequence the number M must be large enough, making the extrapolation to $P \to \infty$ problematic. However, such difficulty can be largely circumvented by making use of our knowledge of both the finite- and infinite-P exact partition function of pure bilinear actions [16]. According to Ref. [16], any PIMC

estimate $G(P)$ of a given quantity G obtained at finite P can be corrected by adding the exact ($P \to \infty$) value $G^{(\mathrm{h})}_{\mathrm{HA}}$ and subtracting the finite-P estimate $G^{(\mathrm{h})}_{\mathrm{HA}}(P)$ of the same quantity. This can be done within the self-consistent harmonic approximation, getting:

$$G_{\mathrm{HA}}(P) = G(P) + \left[G^{(\mathrm{h})}_{\mathrm{HA}} - G^{(\mathrm{h})}_{\mathrm{HA}}(P) \right] \ . \tag{8}$$

As it has been clearly shown in the applications [15], the last step turns out to be essential and truly effective in the investigation of many-body systems.

3. Josephson Junction Arrays

Two-dimensional (2D) JJA are one of the best experimental realizations of a model belonging to the XY universality class and permit to check and study a variety of phenomena related to both the thermodynamics and the dynamics of vortices. In these systems a Berezinskii-Kosterlitz-Thouless (BKT) transition [17] separates the low-temperature superconducting (SC) state from the normal (N) state, the latter displaying no phase coherence [18]. At nanoscale size of the junctions, the quantum fluctuations of the superconducting phases cause new interesting features. These appear to be the consequence of the non-negligible energy cost of charge transfer between SC islands. Indeed small capacitances are involved and the phase and charge are canonically conjugate variables. A relevant effect is the progressive reduction of the SC-N transition temperature as evidenced by experimental data [1] and confirmed for small quantum coupling g (see definition below) by a semiclassical investigation [7].

Recently, arrays of nanosized junctions, both unshunted [1] and shunted [2], have given the opportunity to experimentally approach the quantum (zero-temperature) phase transition. However, the mechanism of suppression of the BKT in the neighborhood of the quantum critical point and its connection with the observed reentrance of the array resistance as function of the temperature is not yet clear [18, 19].

The JJA on the square lattice is described by a quantum XY model action:

$$S[\boldsymbol{\varphi}] = \int_0^{\hbar\beta} \frac{du}{\hbar} \left\{ \sum_{\boldsymbol{ij}} \frac{\hbar^2 C_{\boldsymbol{ij}}}{8e^2} \dot{\varphi}_{\boldsymbol{i}}(u)\, \dot{\varphi}_{\boldsymbol{j}}(u) - \frac{E_{\mathrm{J}}}{2} \sum_{\boldsymbol{id}} \cos \varphi_{\boldsymbol{id}}(u) \right\}, \tag{9}$$

where $\varphi_{\boldsymbol{id}} = \varphi_{\boldsymbol{i}} - \varphi_{\boldsymbol{i}+\boldsymbol{d}}$ is the phase difference between the Josephson phases on the $\boldsymbol{i}$th and the $(\boldsymbol{i}+\boldsymbol{d})$th neighboring superconducting islands, and the index $\boldsymbol{d}$ labels the 4 nearest-neighbour displacements. The capacitance matrix reads

$$C_{\boldsymbol{ij}} = C \left[\eta\, \delta_{\boldsymbol{ij}} + \left(z\, \delta_{\boldsymbol{ij}} - \sum\nolimits_{\boldsymbol{d}} \delta_{\boldsymbol{i},\boldsymbol{j}+\boldsymbol{d}} \right) \right], \tag{10}$$

where $C_0 \equiv \eta\, C$ and C are, the self- and mutual capacitances of the islands respectively. The standard samples of JJA are well decribed by the limits $\eta \ll 1$. The quantum character of the array is determined by the Coulomb interaction between the Cooper pairs, described by the kinetic term through Josephson relation $\dot{\varphi}_{\boldsymbol{i}} = 2eV_{\boldsymbol{i}}$. The Josephson coupling term causes the Cooper-pair tunneling across the junctions.

The quantum fluctuations are ruled by the *quantum coupling* parameter $g = \sqrt{E_{\rm C}/E_{\rm J}}$, where $E_{\rm C} = (2e)^2/2C$ is the characteristic charging energy (for $\eta \ll 1$). In the following we use the *dimensionless temperature* $t \equiv k_{\rm B}T/E_{\rm J}$. We always assume the presence of at least a very weak Ohmic dissipation due to the currents flowing to the substrate or through shunt resistances [2]: this allows us to consider the phase as an extended variable [18]. Apart from this, dissipative effects are negligible provided that the shunt resistance $R_{\rm S} \gg R_{\rm Q}\, g^2/(2\pi t)$, where $R_{\rm Q} \equiv h/(2e)^2$ is the quantum resistance. For smaller $R_{\rm S}$ an explicit dissipative contribution must be added to the action (9), e.g. in the form of the Caldeira-Leggett term [18, 7], as given in (3), where $\varphi_{\boldsymbol{i}}(u)$ play the role of $\boldsymbol{q}_{\boldsymbol{i}}(u)$. The two situations are the cases of the experiments in Ref. [1] and Ref. [2], respectively, where an increase of the BKT transition temperature was found for increasing dissipation. This can be easily understood taking into account that the dissipative term (3) results from the coupling of the phase $\varphi_{\boldsymbol{i}}$ with environmental variables constituting an implicit measurement of $\varphi_{\boldsymbol{i}}$.

4. Numerical simulations and phase diagram

Using the PIMC algorithm described in Sec.2, the dependence on g of the BKT transition temperature of the JJA model described by the action (9) with the additional dissipative term (3) is obtained.

The discretized path can be written as:

$$\varphi_{\boldsymbol{i},l} = \bar{\varphi}_{\boldsymbol{i}} + 2\sum_{k=1}^{N} \Re\mathrm{e}\left[\varphi_{\boldsymbol{i}k}\mathrm{e}^{-i\frac{2\pi}{P}lk}\right] = \bar{\varphi}_{\boldsymbol{i}} + 2\sum_{k=1}^{N}\left[a_{\boldsymbol{i}k}\cos\tfrac{2\pi lk}{P} + b_{\boldsymbol{i}k}\sin\tfrac{2\pi lk}{P}\right], \tag{11}$$

where $\bar{\varphi}_{\boldsymbol{i}}$ is the zero-frequency component of the Euclidean path, and choosing an odd Trotter number $P = 2N + 1$. The advantage of using the transformed variables $\{\bar{\varphi}_{\boldsymbol{i}}, a_{\boldsymbol{i}k}, a_{\boldsymbol{i}k}\}$ is twofold: the influence action (3) becomes diagonal and PIMC sampling can be performed with an independent move amplitude on each frequency component.

Using expression (11), the JJA action (9) plus the dissipative term (3) reads

$$S[\boldsymbol{\varphi}] = \sum_{\boldsymbol{ij}}\sum_{k=1}^{N} T_{\boldsymbol{ij},k}(a_{\boldsymbol{i}k}a_{\boldsymbol{j}k} + b_{\boldsymbol{i}k}b_{\boldsymbol{j}k}) - \frac{1}{2Pt}\sum_{\boldsymbol{id}}\sum_{l=1}^{P}\cos\varphi_{\boldsymbol{ij},l}\,, \tag{12}$$

where $\varphi_{\boldsymbol{ij},l} = \varphi_{\boldsymbol{i},l} - \varphi_{\boldsymbol{j},l}$ is to be expressed as in (11), and the 'kinetic' matrix

$$T_{\boldsymbol{ij},k} = \frac{P^2}{\beta e^2} C_{\boldsymbol{ij}} \sin^2 \frac{\pi k}{P} + \beta K_{\boldsymbol{ij},k} \,, \tag{13}$$

involves $K_{\boldsymbol{ij},k}$, i.e., the discrete FT of the dissipative kernel matrix $K_{\boldsymbol{ij}}(u)$. Any macroscopic thermodynamic quantity is obtained through its estimator as generated from the discretized action (12).

Actual simulations were made on $L \times L$ lattices (up to $L = 96$) with periodic boundary conditions; the move amplitudes were dynamically adjusted for each k-component; this procedure is very effective for reproducing the effect of strong quantum fluctuations in the high-g region, at difference with the standard PIMC algorithm which showed serious ergodicity problems, though eventually giving the same results. Furthermore, an over-relaxation algorithm [22] for the zero-frequency mode proved to effectively reduce the autocorrelation times.

In order to determine the transition temperature, a very sensitive method is provided by the scaling law of the helicity modulus Υ (a quantity proportional to the phase stiffness),

$$\Upsilon = \left(\frac{\partial^2 f(k_0)}{\partial k_0^2} \right)_{k_0 = 0} \,, \tag{14}$$

which measures the response of the dimensionless free energy per lattice site $f(k_0) = F(k_0)/(L^2 \, E_{\mathrm{J}})$ when a uniform twist k_0 along a fixed direction $\boldsymbol{u}$ is applied to the boundary conditions (i.e., $\varphi_{\boldsymbol{i}} \to \varphi_{\boldsymbol{i}} + k_0 \boldsymbol{u} \cdot \boldsymbol{i}$, with the unitary vector $\boldsymbol{u}$). The PIMC estimator for Υ is easily obtained, in analogy to that of Ref. [23], by derivation of the discretized path-integral expression of the free energy

$$f(k_0) = \frac{t}{L^2} \, \ln Z_P(k_0) \tag{15}$$

Eventually we get

$$\Upsilon_P = \frac{1}{L^2 P} \sum_{\boldsymbol{id}} \sum_{l=1}^{P} \cos \varphi_{\boldsymbol{id},l} - \frac{1}{2 t L^2 P^2} \sum_{\boldsymbol{d}} \left(\sum_{\boldsymbol{i}} \sum_{l=1}^{P} \sin \varphi_{\boldsymbol{id},l} \right)^2 . \tag{16}$$

Kosterlitz's renormalization group equations provide the critical scaling law for the finite-size helicity modulus Υ_L:

$$\frac{\Upsilon_L(t_{\mathrm{BKT}})}{t_{\mathrm{BKT}}} = \frac{2}{\pi} \left(1 + \frac{1}{2 \ln(L/L_0)} \right) \,, \tag{17}$$

where L_0 is a non-universal constant. Following Ref. [24], the critical temperature t_{BKT} can be found by fitting $\Upsilon_L(t)/t$ vs L for several temperatures

according to Eq. (17) with a further multiplicative fitting parameter $A(t)$. In this way, the critical point can be determined by searching the temperature such that $A(t_{\rm BKT}) = 1$, getting results like those reported in Fig 1. This method allows for a precise identification of $t_{\rm BKT}$: at temperature higher (lower) than the critical one the helicity modulus decreases (increases) much faster with L than $\Upsilon_L(t_{\rm BKT})$. At higher values of the quantum coupling, $g > g^\star$, the helicity modulus scales to zero with $L \to \infty$ and $P \to \infty$ at any temperature [21].

Systematic extrapolations in the Trotter number and in the lattice size have been done, in order to ascertain the good approach to the quantum and the thermodynamic limit. In particular, we did not find any anomaly in the finite-P behavior: the extrapolations in the Trotter number appear to be well-behaved, in the expected asymptotic regime $\mathcal{O}(1/P^2)$ [26], for $P \sim 60$. Moreover, the extrapolation to infinite lattice-size clearly indicates that Υ_L scales to zero at $t = 0.1$, while it remains finite and *sizeable* at $t = 0.2$. Therefore, we conclude that the reentrant behavior of the helicity modulus appears to be a genuine effect present in the model, rather than a finite-Trotter or finite-size artifact.

5. Discussion of the results

In order to understand the physical reasons of the reentrance observed in the phase stiffness, we have studied the following two quantities:

$$\left\langle \cos\, \varphi_{\boldsymbol{ij}} \right\rangle , \qquad \Delta^2_\varphi = \left\langle \, (\varphi_{\boldsymbol{ij}}(u) - \bar{\varphi}_{\boldsymbol{ij}})^2 \, \right\rangle , \tag{18}$$

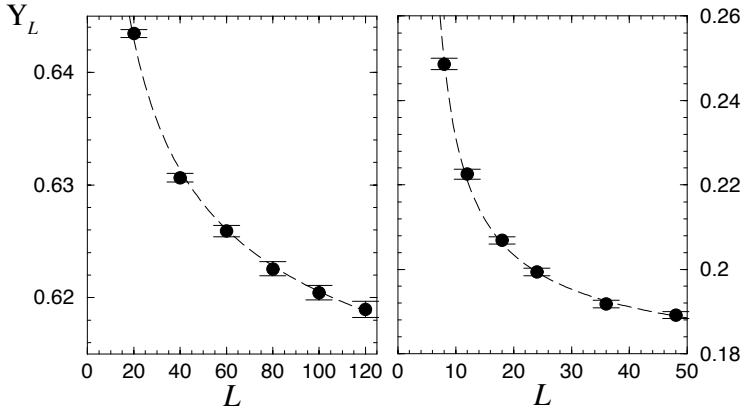

Figure 1. Size scaling of the helicity modulus Υ_L at the transition temperature. Symbols are PIMC data and the dashed-lines are the one-parameter fit with Eq. (17), i.e. with $A(t) = 1$. Left panel: $g = 0$ and $t = 0.892$ [$L_0 = 0.456(6)$]; right panel: $g = 3.4$ and $t = 0.25$ [$L_0 = 3.32(3)$].

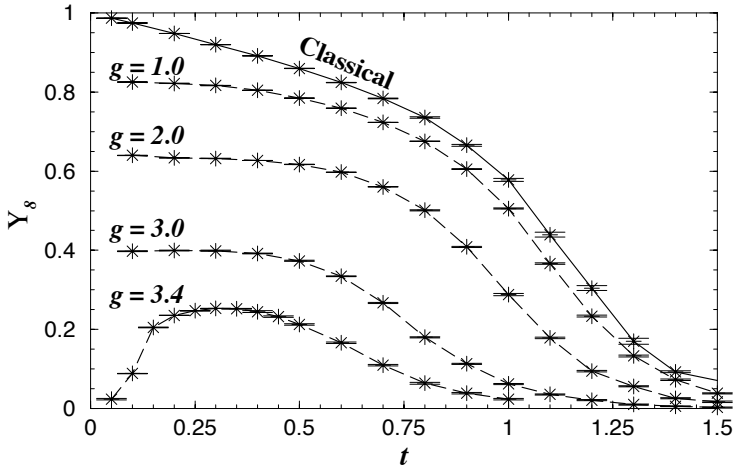

Figure 2. Temperature behavior of the helicity modulus Υ_L at selected values of coupling g. The data are the results for $8\,x\,8$ lattice with Trotter extrapolation.

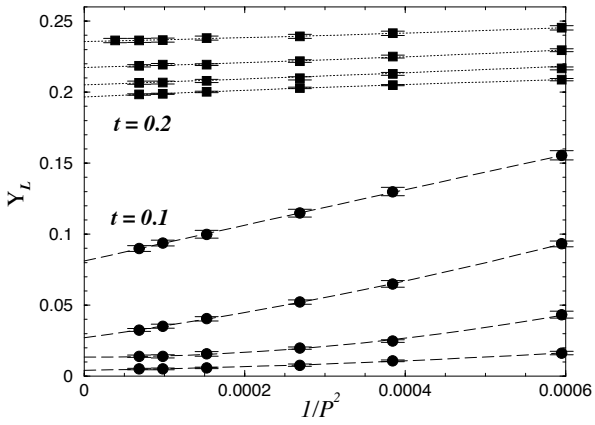

Figure 3. Trotter extrapolation of helicity modulus for $g = 3.4$.

where $\bar{\varphi}_{ij}$ is the phase average on the imaginary path, being ij nearest-neighbor sites. The first quantity, $\langle \cos \varphi_{ij} \rangle$, is a measure of the total (thermal plus quantum) short-range fluctuations of the Josephson phase and its maximum occurs where the overall fluctuations are lowest. The second quantity represents instead the pure-quantum spread of the phase difference between two neighboring islands and has been recently studied in the single junction problem [27]; more precisely, Δ^2_φ measures the fluctuations around the static value (i.e., the zero-frequency component of the Euclidean path), it is maximum at $t = 0$ and tends to zero in the classical limit, i.e., $(g/t) \to 0$.

The quantities (18) on a 8×8 lattice are compared in Fig. 6 for two values of the quantum coupling, in the semiclassical ($g = 1.0$) and in the extreme quantum ($g = 3.4$) regime. In the first case $\langle \cos \varphi_{ij} \rangle$ decreases monotonically by increasing t and the pure-quantum phase spread Δ^2_φ shows a semiclassical linear behavior which is correctly described by the PQSCHA. At variance with this, at $g = 3.4$, where the reentrance of $\Upsilon(t)$ is observed, $\langle \cos \varphi_{ij} \rangle$ shows a pronounced maximum at finite temperature. Besides the qualitative agreement with the mean-field prediction of Ref. [28], we find a much stronger enhancement of the maximum above the $t = 0$ value. This single-junction effect, in a definite interval of the quantum coupling ($3.2 < g < 3.4$), is so effective to drive the reentrance of the phase stiffness. As for the transition in the region of high quantum fluctuations and low temperature, the open symbols in Fig. 5 represent the approximate location of the points (t, g) where $\Upsilon(t)$ becomes zero within the error bars: in their neighborhood we did not find any BKT-like scaling law. This fact opens two possible interpretations: (i) the transition does not belong to the XY universality class; (ii) it does, and in this case the control parameter is not the (renormalized) temperature, but a more involute function of both t and g.

When the interaction of the phase variable with a heat bath, as given by Eq. (3), is present through a variable shunt resistance, the quantum phase fluctuations are decreased by the dissipation so that the BKT transition temperature rises. This was well reproduced by PQSCHA at low coupling [7].

Two points must be noticed. The reentrance is present also with dissipation and disappears only with rather significant dissipation strength $R_Q/R_S \sim 0.15$. At the highest dissipation, $R_Q/R_S > 0.5$, a change in curvature is present and the critical temperature asymptotically vanishes.

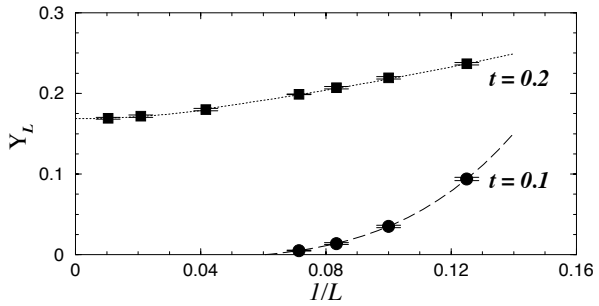

Figure 4. Finite size scaling of helicity modulus for $g = 3.4$ at $P = 101$.

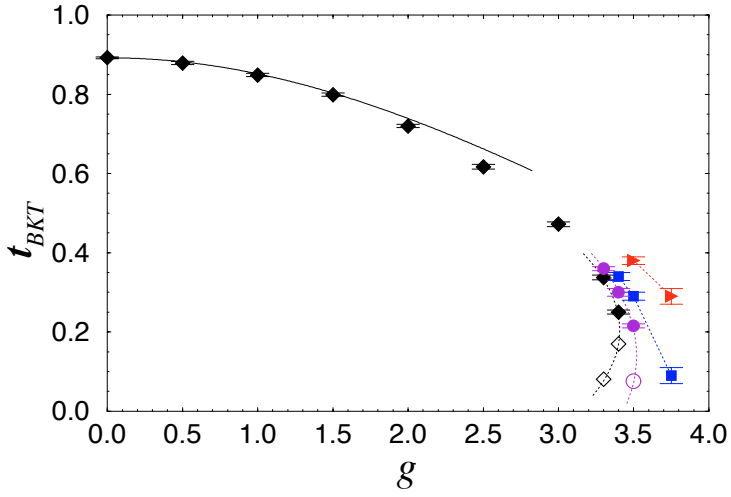

Figure 5. Phase diagramm. BKT transition temperatures versus coupling g. Full rhombs represent the BKT transition temperatures for very low dissipations compared with the semi-classical approach (full line). The full circles refer different intensities of the dissipation from $R_Q/R_S = 0.15$ (lowest), $R_Q/R_S = 0.25$ and $R_Q/R_S = 0.15$ (highest). Open circles refer to reentrance phenomena for vanishing and $R_Q/R_S = 0.15$ dissipation .

Acknowledgments

Fruitful discussions with G. Falci, R. Fazio and F.Guinea are gratefully acknowledged. We acknowledge support by INFN, INFM, and MIUR-COFIN2002.

References

[1] H. S. J. van der Zant, W. J. Elion, L. J. Geerligs and J. E. Mooij, Phys. Rev. B **54**, 10081 (1996).

[2] Y. Takahide, R. Yagi, A. Kanda, Y. Ootuka, and S. Kobayashi, Phys. Rev. Lett. **85**, 1974 (2000).

[3] A. O. Caldeira and A. J. Leggett, Ann.Phys. (NY) **149**, 374 (1983).

[4] G. W. Ford, M. Kac and P. Mazur, J. Math. Phys. **6**, 504 (1965).

[5] see for instance: U. Weiss, *Quantum Dissipative Systems*, World Scientific, II ed. Singapore 1999

[6] A. Cuccoli, A. Fubini, V. Tognetti, and R. Vaia, Phys. Rev. B **60**, 231 (1999).

[7] A. Cuccoli, A. Fubini, V. Tognetti, and R. Vaia, Phys. Rev. B **61**, 11289 (2000).

[8] F. Sols and I. Zapata, in *New Developments on Fundamental Problems in Quantum Physics*, ed. by M. Ferrero and A. van der Merwe (Kluver, Dordrecht, 1997).

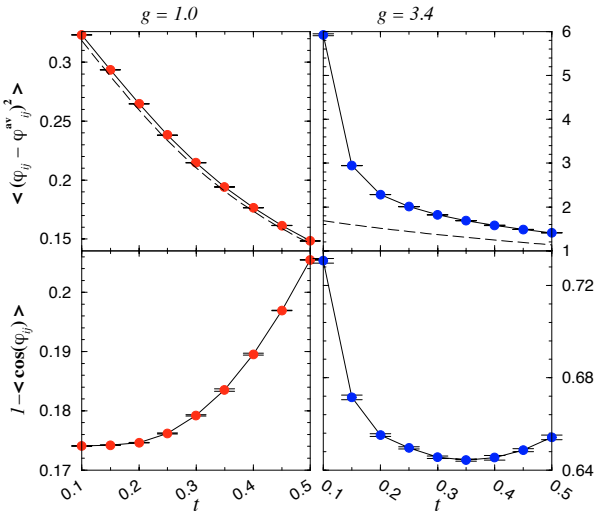

Figure 6. Behaviour of fluctuations at different values of coupling. Full circles refer to PIMC calculations. Dashed lines are the semiclassic results.

[9] Yu. Makhlin, G. Schoen and A. Shnirman in *New Directions in Mesoscopic Physics*, eds. R. Fazio, V.F. Gantmakher, Y. Imry (Kluver, Dordrecht, 2003).

[10] A.Leggett, Phys. Rev. B bf 30, 1208 (1884).

[11] A. Cuccoli, A. Fubini, V. Tognetti, and R. Vaia, Phys. Rev. E **64**, 066124-1 (2001).

[12] R. Giachetti and V. Tognetti, Phys. Rev. Lett. **55**, 912, (1985).

[13] J. D. Doll and D. L. Freeman, J. Chem. Phys. **80**, 2239, (1984).

[14] M. Eleftheriou, J. D. Doll, E. Curotto and D. L. Freeman, J. Chem. Phys. **110**, 6657, (1999).

[15] L. Capriotti, A. Cuccoli, A. Fubini, V. Tognetti and R. Vaia, Europhys. Lett. **58**, 155, (2002)

[16] A. Cuccoli, A. Macchi, A. G. Pedrolli, V. Tognetti, and R. Vaia, Phys. Rev. B, **51**, 12369, (1995).

[17] V. L. Berezinskii, Zh. Eksp. Teor. Fiz. **59**, 907 (1970) [Sov. Phys. JEPT **32**, 493 (1971)]; J. M. Kosterlitz and D. J. Thouless, J. Phys. C **6**, 1181 (1973).

[18] R. Fazio and H. S. J. van der Zant, Phys. Rep. **355**, 235 (2001).

[19] H. M. Jaeger, D. B. Haviland, B. G. Orr, and A. M. Goldman, Phys. Rev. B **40**, 182 (1989).

[20] L. Capriotti, A. Cuccoli, A. Fubini, V. Tognetti, and R. Vaia, Europhys. Lett. **58**, 155 (2002).

[21] L. Capriotti, A. Cuccoli, A. Fubini, V. Tognetti, and R. Vaia, Phys. Rev. Lett. **91**, 247004 (2004).

[22] F. R. Brown and T. J. Woch, Phys. Rev. Lett. 58, 2394 (1987).

[23] C. Rojas and J. V. Jose, Phys. Rev. B **54**, 12361 (1996). (1994).

[24] K. Harada and N. Kawashima, J. Phys. Soc. Jpn. **67**, 2768 (1998); A. Cuccoli, T. Roscilde, V. Tognetti, R. Vaia, and P. Verrucchi, Phys. Rev. B **67**, 104414 (2003).

[25] P. Olsson, Phys. Rev. Lett. 73, 3339 (1994); M. Hasenbusch and K. Pinn, J. Phys. A 30, 63 (1997); S. G. Chung, Phys. Rev. B **60**, 11761 (1999).

[26] M. Suzuki, *Quantum Monte Carlo methods in equilibrium and nonequilibrium systems*, ed. M. Suzuki (Springer-Verlag, Berlin, 1987).

[27] C. P. Herrero and A. Zaikin, Phys. Rev. B **65** 104516 (2002).

[28] P. Fazekas, B. Muhlschlegel, and Schroter, Z. Phys. B **57**, 193 (1984).